Evolution on Structural Stability and Morphological Studies of Neodymium-Doped $LiMn_{1.9}Ti_{0.1}O_4$ Spinel Cathodes for Lithium-Ion Batteries

M.H.H. Mokhtar[1], S.A.F. Bakri[1], I. Buniyamin[2], N.A.M. Makhatar[3], A.F.M. Fadzil[4*]

[1-4]Universiti Teknologi MARA, Malaysia
✉ Corresponding email: aidafazliza@uitm.edu.my

History of Article
Submitted : July 18, 2026
Revised : July 25, 2026
Accepted : August 10, 2026
Published : September 22, 2026
DOI : https://doi.org/10.37253/conescintech.v6i1.12703

Copyright© 2026 by Author(s). This work is licensed under a Creative Commons Attribution-Non Commercial-Share Alike 4.0 International License. All writings published in this journal are personal views of the authors and do not represent the views of this journal and the author's affiliated institutions.

Abstract
The spinel-structured material $LiMn_2O_4$ (LMO) has attracted attention for its good rate capability but suffers from capacity fading, manganese dissolution, and poor stability at high temperatures. Partial doping with other elements is an effective strategy to address these issues. To identify suitable dopant ratios for potential cathode material, the structural and morphological is studied through rare-earth doping with Neodymium (x=0.01 and x=0.05) using the Self-Propagating Combustion (SPC) method. X-ray diffraction (XRD) confirmed a single-phase cubic spinel formation without structural disorder. The XRD profiles show a very good fit between the observed and the database. The obtained samples were identified as single-phase spinel with a face-centered cubic (FCC) structure. The XRD data also indicate that Nd doping does not affect the formation of the cubic spinel structure of $LiMn_{1.9}Ti_{0.1}O_4$. Annealing at 800 °C for 24 hours causes an increase in sample crystallinity. Scanning Electron Microscope (SEM) and Energy Dispersive X-ray Spectroscopy (EDX) analyses showed uniformly distributed polyhedral particles ranges from 250nm to 450nm, with homogeneous distribution of Mn, Ti, Nd, and O. The synergy of advanced materials science results in a highly accelerated, scalable process for designing potential high-performance, upcoming-generation lithium-ion batteries.

Keywords: $LiMnTiO_4$; Rare-earth; Neodymium; Combustion; Lithium-Ion Batteries

Introduction

The rapid expansion of electric vehicles and renewable energy storage systems has created a demand for high-performance lithium-ion batteries (LIBs) with high energy density, cycling stability, and safety (Hebert & McCalla, 2021; Lin et al., 2026). Spinel

lithium manganese oxide $LiMn_2O_4$ (LMO) is a potential cathode material for its low cost, environmental friendliness, high working voltage, and three-dimensional lithium-ion diffusion pathways (Huang et al., 2021; Thackeray, 2021; Y. Zhang et al., 2020).

Rare earth elements are interesting dopants due to their large ionic radii and capacity to impact crystal formation and lattice stability. Neodymium (Nd^{3+}) has the potential to improve crystallinity, change particle shape, and strengthen the structural integrity of spinel cathodes (Balaji et al., 2012; Wang, L. et al., 2023; Zybert et al., 2023). However, limited research has been conducted on Nd-substituted $LiMn_{1.9}Ti_{0.1}O_4$ materials, especially those synthesized utilizing the Self-Propagating Combustion (SPC) process. Furthermore, the effect of various Nd concentrations on phase formation and morphological properties has not been thoroughly studied. This study addresses this gap by examining Nd substitution in SPC-synthesized $LiMn_{1.9}Ti_{0.1}O_4$ cathodes.

This paper studies how neodymium substitution affects the structural stability and morphology of $LiMn_{1.9}Ti_{0.1}O_4$ spinel cathodes produced using the SPC method and annealed at 800 °C for 24 hours. The compositions are $LiMn_{1.9}Ti_{0.1}O_4$, $LiMn_{1.9}Ti_{0.09}Nd_{0.01}O_4$, and $LiMn_{1.9}Ti_{0.05}Nd_{0.05}O_4$. The samples were analyzed using X-ray diffraction (XRD), scanning electron microscopy (SEM), and energy-dispersive X-ray spectroscopy (EDX). The results focus on the interaction between Nd inclusion, crystal structure, and particle morphology, which will help to design structurally stable cathode materials for enhanced lithium-ion battery applications and clarify the effect of Nd concentration that remains insufficiently explored.

Research Method

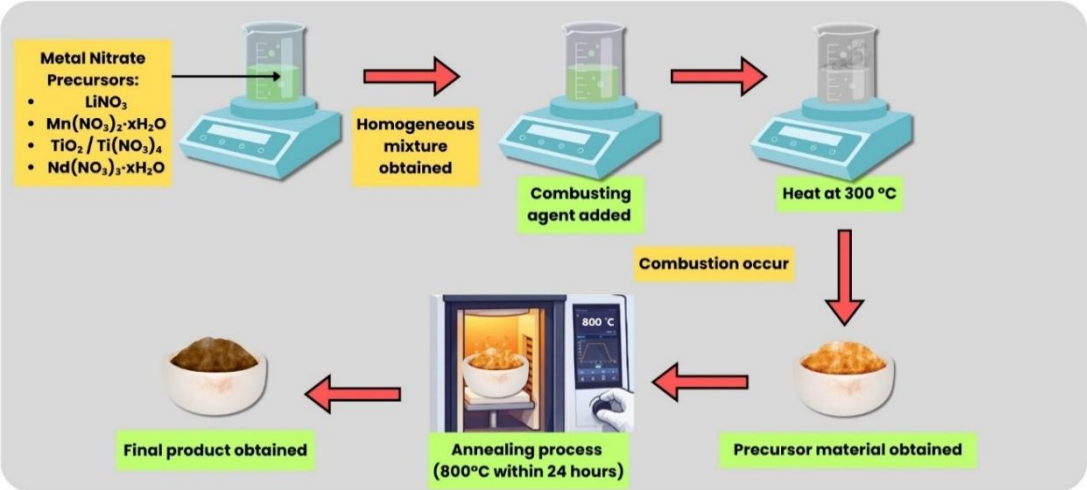
Research Design

This study used a quantitative experimental approach to evaluate how neodymium (Nd) substitution affects the structural stability and morphological properties of Ti-doped lithium manganese oxide spinel cathodes. Three compositions, $LiMn_{1.9}Ti_{0.1}O_4$ (LMT), $LiMn_{1.9}Ti_{0.09}Nd_{0.01}O_4$ (LMTN-01), and $LiMn_{1.9}Ti_{0.05}Nd_{0.05}O_4$ (LMTN-05) were synthesized and compared. To determine the influence of increasing Nd concentration on the crystal structure and particle morphology of spinel cathode materials, all samples were synthesized under similar synthesis and annealing conditions.

Synthesis of Cathode Materials

The cathode materials were prepared utilizing the Self-Propagating Combustion (SPC) process, as shown in Figure 1. To create a homogenous solution, lithium nitrate ($LiNO_3$), manganese nitrate hydrate [$Mn(NO_3)_2 \cdot xH_2O$], titanium precursor, and neodymium nitrate hydrate [$Nd(NO_3)_3 \cdot xH_2O$] were dissolved in deionized water with

constant stirring. A suitable combustion agent was then introduced into the precursor solution and carefully stirred until a homogenous mixture formed.



A self-sustaining combustion reaction was initiated by heating the produced gel to around 300 °C. The precursor decomposed quickly during combustion, resulting in a porous powder precursor (Zhang, Y. et al., 2021). The powders were milled uniformly and placed in alumina crucibles for heat treatment.

The powders were then annealed in a furnace at 800 °C for 24 hours at ambient atmosphere conditions to facilitate crystallization and phase development of the spinel structure. Following annealing, the samples were naturally cooled to room temperature before being kept for further analysis.

Structural Characterisation

X-ray diffraction (XRD) using Cu-Kα radiation (λ = 1.5406 Å) was used to evaluate the crystal structure and phase purity of the produced samples. Diffraction data were obtained throughout a 2θ range of 10° to 90°. The resulting diffraction patterns were utilized to identify the crystalline phases, determine phase purity, and assess the structural integrity of the spinel framework following Nd substitution (Llewellyn et al., 2020).

Morphological and Elemental Characterisation

The surface appearance and particle properties of the produced powders were studied using scanning electron microscopy (SEM). SEM analysis was used to obtain particle shape, distribution, grain formation, and morphological evolution at various Nd concentrations.

The energy-dispersive X-ray spectroscopy (EDX) linked to the SEM equipment was used to evaluate the elemental composition and distribution. EDX measurements were used to confirm the presence and homogeneous distribution of Mn, Ti, Nd, and O in the synthesized materials.

Data Analysis

The XRD patterns were compared to standard reference data to confirm the cubic spinel phase development and determine phase purity. Characteristic diffraction peaks were indexed using the spinel crystal structure, and the diffraction profiles of all compositions were carefully examined to determine the effect of Nd inclusion on structural stability.

SEM micrographs were studied to determine particle morphology, particle size distribution, and grain properties. EDX spectra and elemental mapping findings were utilized to confirm elemental composition and evaluate the distribution of constituent elements across the samples.

The evolution of $LiMn_{1.9}Ti_{0.1}O_4$ spinel cathodes with increasing neodymium content was analyzed using structural, morphological, and compositional data from XRD, SEM, and EDX characterizations.

Results and Discussions

Structural Analysis of Nd-Doped $LiMn_{1.9}Ti_{0.1}O_4$ Spinel Cathodes by X-Ray Diffraction (XRD)

The X-ray diffraction (XRD) patterns of the synthesized and annealed at 800 °C for 24 hours, $LiMn_{1.9}Ti_{0.1}O_4$ (LMT), $LiMn_{1.9}Ti_{0.09}Nd_{0.01}O_4$ (LMTN-01), and $LiMn_{1.9}Ti_{0.05}Nd_{0.05}O_4$ (LMTN-05) are shown in Figure 2. The diffraction patterns of all compositions show well-defined crystalline peaks, which suggest the successful production of highly crystalline spinel materials.

The diffraction peaks located at approximately 18.7°, 36.2°, 44.1°, 58.3°, 64.3°, 67.2°, 76.0°, and 81.1° correspond to the (111), (311), (400), (511), (440), (531), (533), and (444) crystallographic planes, respectively. These reflections are typical for the cubic spinel $LiMn_2O_4$ structure in the face-centered cubic (FCC) crystal system with the space group $Fd\bar{3}m$ (Huang et al., 2021; Thackeray, 2021). The diffraction pattern obtained was consistent with the reported spinel $LiMn_2O_4$ cathode materials, which indicates the successful formation of the desired spinel framework.

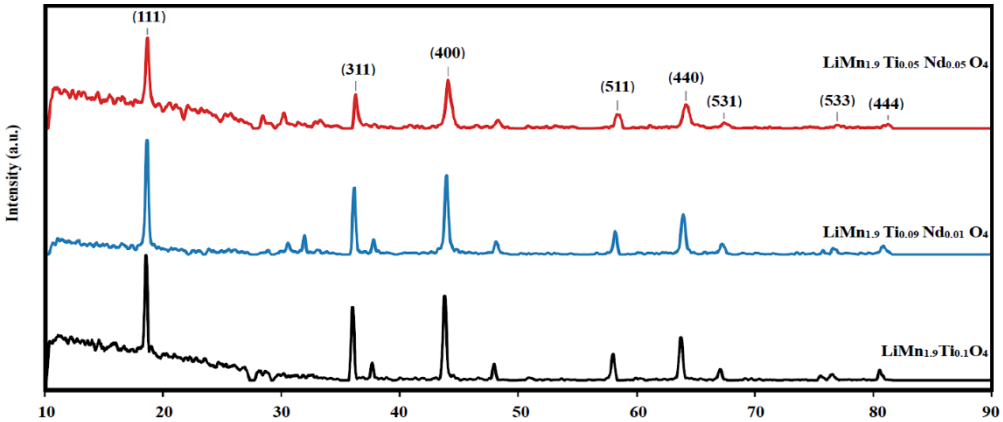


Figure 2. Stacked XRD patterns of $LiMn_{1.9}Ti_{0.1}O_4$ (LMT), $LiMn_{1.9}Ti_{0.09}Nd_{0.01}O_4$ (LMTN-01), and $LiMn_{1.9}Ti_{0.05}Nd_{0.05}O_4$ (LMTN-05) annealed at 800 °C for 24 hours.

E-ISSN: 2808-5485
Available online at website: https://journal.uib.ac.id/index.php/conescintech/index

The comparison of diffraction profiles shows that all characteristic peaks are preserved after neodymium substitution. There is no significant peak splitting or disappearance of the major reflections, suggesting that the crystal symmetry of the Ti-doped $LiMn_2O_4$ host lattice is not changed by the incorporation of the Nd. In addition, no impurity peaks from Nd_2O_3, TiO_2, Mn_2O_3, Mn_3O_4, and other secondary phases are detected in the explored 2θ range. The obtained result confirms that the selected Nd concentrations were well accommodated without disturbing the phase purity of the spinel.

For each composition, the (111) plane exhibits the highest diffraction intensity of all of the reflections measured, indicating that crystal growth occurs preferentially along this crystallographic direction. The synthesized materials display good structural ordering and a high degree of crystallinity, as evidenced by the narrow diffraction profile of the (111) peak and its high intensity. The same properties have been observed in highly crystalline spinel $LiMn_2O_4$ systems produced at high annealing temperatures (Vu et al., 2020; Zhang, Y. et al., 2021).

The diffraction peaks of the Nd-containing samples also remain clear and distinct, suggesting that the annealing temperature of 800 °C was effective at promoting crystal formation and reducing lattice defects. For lithium-ion battery cathodes, higher crystallinity is desirable since it helps to enhance structural stability and lithium-ion diffusion during repeated electrochemical cycling (Huang et al., 2021; Nyamaa et al., 2024).

Although the ionic radius of Nd^{3+} is larger than that of the octahedral site ions of the spinel structure, the XRD data reveal that Nd can be incorporated up to x = 0.05 without producing any observable phase alteration. This preservation of the cubic spinel framework is particularly noteworthy as one of the key prerequisites for achieving improved cycling durability in lithium-ion battery cathode materials is the structural stability of the host lattice when doped with low levels of rare-earth ions, and this has been demonstrated. (Kumar et al., 2022; Ram et al., 2016).

According to the XRD study, all synthetic compositions have a single-phase cubic spinel structure with good crystallinity and excellent phase stability. The successful retention of the $Fd\bar{3}m$ spinel framework after Nd substitution indicates that rare-earth elements can be incorporated into Ti-doped $LiMn_2O_4$ without compromising the framework stability of the battery materials, highlighting the potential of Nd modification as a strategy for creating structurally stable materials for lithium-ion batteries (Kumar et al., 2022; Nyamaa et al., 2024).

Morphological Evolution of Nd-Doped $LiMn_{1.9}Ti_{0.1}O_4$ Spinel Cathodes by Scanning Electron Microscope (SEM)

SEM was used to analyze the surface morphology of $LiMn_{1.9}Ti_{0.1}O_4$ (LMT), $LiMn_{1.9}Ti_{0.09}Nd_{0.01}O_4$ (LMTN-01), and $LiMn_{1.9}Ti_{0.05}Nd_{0.05}O_4$ (LMTN-05) at magnifications of 1000× and 10000×. Comparable SEM micrographs are presented in Figure 3, with average particle sizes summarized in Table 1. The average particle size was

calculated by determining the mean value of the diameters of five representative particles using the following equation:

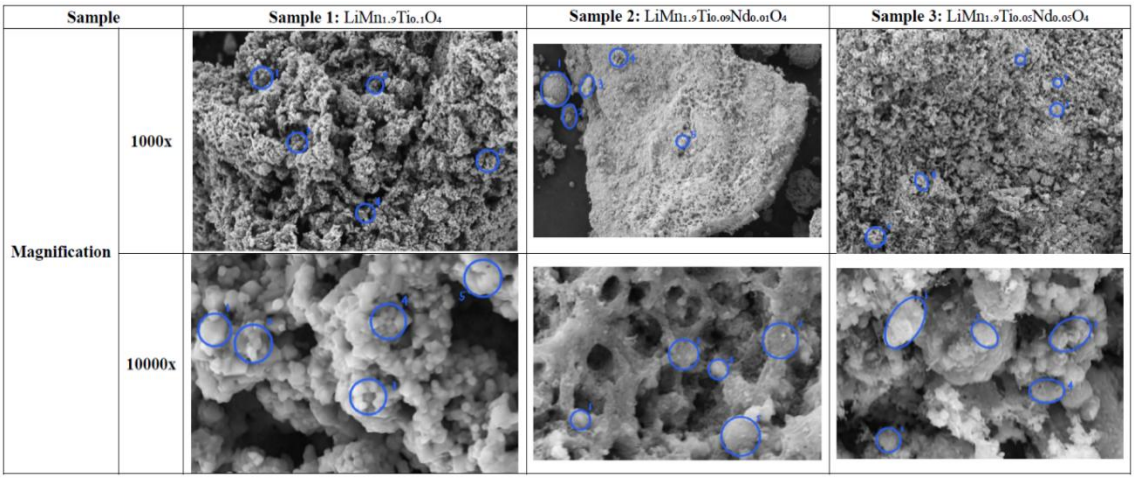


Figure 3. SEM images of $LiMn_{1.9}Ti_{0.1}O_4$ (LMT), $LiMn_{1.9}Ti_{0.09}Nd_{0.01}O_4$ (LMTN-01), and $LiMn_{1.9}Ti_{0.05}Nd_{0.05}O_4$ (LMTN-05) spinel cathodes showing the effect of Nd doping on particle morphology and agglomeration at 1000× and 10000× magnifications.

Table 1. Average particle size of $LiMn_{1.9}Ti_{0.1-x}Nd_xO_4$ samples obtained from SEM analysis.

Sample	Magnification	Particle 1 (µm)	Particle 2 (µm)	Particle 3 (µm)	Particle 4 (µm)	Particle 5 (µm)	Average Particle Size (µm)
Sample 1: $LiMn_{1.9}Ti_{0.1}O_4$	**10000x**	0.77	0.90	0.84	0.84	0.89	**0.848**
Sample 2: $LiMn_{1.9}Ti_{0.09}Nd_{0.01}O_4$	**10000x**	0.43	0.85	0.73	0.46	0.93	**0.680**
Sample 3: $LiMn_{1.9}Ti_{0.05}Nd_{0.05}O_4$	**10000x**	0.65	0.24	0.36	0.58	0.53	**0.472**

For each SEM micrograph, five typical particles were chosen, and the mean particle size was calculated based on an image scale conversion ratio of 1 cm = 1 µm. The particle size decreased progressively and significantly over the three samples in a comparison study at 10000X magnification. The largest average grain diameter is for the sample LMT, at 0.848 µm. However, a small proportion of LMTN-01 has been replaced with rare-earth, decreasing particle size to 0.680 µm, which is 19.81% smaller than LMTN-01 without the substitution. By increasing the substitution percentage to 50% in the LMTN-05 sample, the grain growth was decreased to 0.472 µm, which is a 44.34% decrease from the pure LMT sample, and an increase of 30.59% more particle refinement has been achieved than compared directly with the LMTN-01 sample. A comparable decrease in the average particle size was maintained for the 1000× magnification with an average of 0.448 µm (LMT) compared with 0.252 µm (LMTN-05), equivalent to a total reduction of 43.75%. This quantitative trend shows that as the amount of neodymium

substitution gets higher, the number of grain boundaries decreases and the structure of the framework becomes more refined exponentially.

The introduction of Nd^{3+} into the spinel lattice leads to the introduction of localized strain and pinning of the grain boundaries, restricting the atomic diffusion and preventing excessive crystal growth during annealing (Zhou et al., 2024). With higher Nd content, finer and more evenly distributed particles are formed.

Smaller particles are advantageous to electrochemistry because they have shorter lithium-ion diffusion paths and larger electrode-electrolyte interfaces (Huang et al., 2021; Nyamaa et al., 2024). These properties are optimized for Li^+ transport, reaction kinetics, and utilization of the active material during charge-discharge cycles. In addition, the clean microstructures could improve the electrolyte penetration and could increase the electrochemically active surface area.

The morphological refinement observed in Nd doped samples gives support to the conclusion of structural stability as established by XRD investigation. Smaller particle sizes can help to decrease internal mechanical stress during lithium insertion and extraction, minimizing structural degradation (Pei et al., 2024; Y. Zhang et al., 2021). Moreover, the lattice stabilization effect of the strong interaction between Nd and oxygen is also believed to help to suppress the Jahn-Teller distortion for Mn^{3+}.

The composition with the highest Nd incorporation, LMTN-05, shows the highest grain-growth suppression and the smallest average particle size, suggesting that greater control of the microstructural development can be obtained by increasing the Nd incorporation. The morphology of Ti-doped $LiMn_2O_4$ spinel cathodes is enhanced by refinement of the particles and improved structural stability of Nd substitution (Wang, Y. et al., 2026; Zhou et al., 2024).

As shown in the SEM result, the microstructure of $LiMn_{1.9}Ti_{0.1}O_4$ changed with increasing Nd content, leading to smaller particles and a more uniform distribution. The morphological modifications improve lithium-ion diffusion and structural resistance, making Nd-doped $LiMn_{1.9}Ti_{0.1}O_4$ a promising cathode material for advanced lithium-ion batteries application.

Compositional and Elemental Distribution Analysis by Energy-Dispersive X-ray Spectroscopy (EDX)

Energy-Dispersive X-ray Spectroscopy (EDX) was used to study the elemental composition and spatial distribution of the synthesized cathode materials, $LiMn_{1.9}Ti_{0.1}O_4$ (LMT), $LiMn_{1.9}Ti_{0.09}Nd_{0.01}O_4$ (LMTN-01), and $LiMn_{1.9}Ti_{0.05}Nd_{0.05}O_4$ (LMTN-05), and elemental mapping analysis was performed. The EDX spectra and elemental distribution maps are shown in Figure 4.

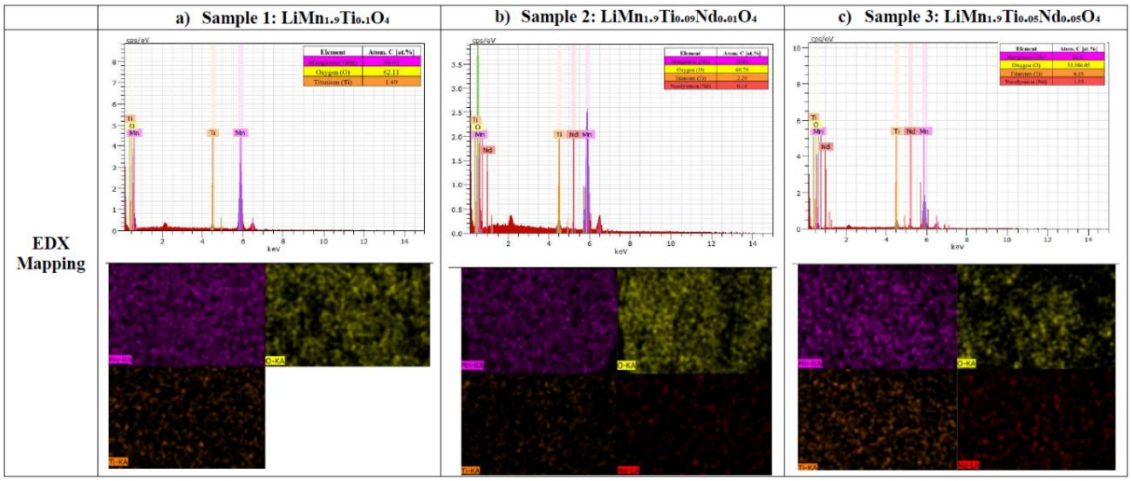


Figure 4. EDX spectra of a) $LiMn_{1.9}Ti_{0.1}O_4$ (LMT), b) $LiMn_{1.9}Ti_{0.09}Nd_{0.01}O_4$ (LMTN-01), and c) $LiMn_{1.9}Ti_{0.05}Nd_{0.05}O_4$ (LMTN-05) spinel cathode materials showing the presence of Mn, Ti, Nd, and O elements.

The spectrum of EDX for the pristine sample of LMT shows characteristic peaks of manganese (Mn), titanium (Ti), and oxygen (O), which indicates that the spinel of Ti-doped lithium manganese oxide material was successfully formed. No additional impurity-related peaks were detected, indicating good chemical purity of the synthesized sample. The other peaks, which could be attributed to neodymium (Nd), were clearly observed for the Nd-containing compositions, namely LMTN-01 and LMTN-05. The elemental composition and spatial distribution of the produced cathode materials $LiMn_{1.9}Ti_{0.1}O_4$ (LMT), $LiMn_{1.9}Ti_{0.09}Nd_{0.01}O_4$ (LMTN-01), and $LiMn_{1.9}Ti_{0.05}Nd_{0.05}O_4$ (LMTN-05) were analyzed using Energy-Dispersive X-ray Spectroscopy (EDX). The EDX spectra and corresponding elemental distribution maps are presented in Figure 4.

The EDX spectrum of the as-prepared LMT sample exhibits characteristic peaks of manganese (Mn), oxygen (O), and titanium (Ti) elements, confirming the synthesis of Ti-doped $LiMn_2O_4$ spinel material. No more impurity-related peaks were observed, indicating that the produced material is chemically pure. The Nd-containing compositions (LMTN-01 and LMTN-05) showed clearly visible additional neodymium (Nd) peaks.

The LMTN-05 sample also contains all of the intentional elements, suggesting successful Nd synthesis at higher doping levels. The elemental maps, however, indicate a much higher concentration of Ti and Nd than the surrounding matrix in certain locations. The data indicate that the element distribution is less uniform with higher Nd content, possibly due to local enrichment of elements during crystal formation and thermal processing. However, there were no distinguishable impurity phases in the XRD test, maintaining the overall cubic spinel structure.

The measured transition-metal to oxygen ratio is very close to the spinel value, suggesting that oxygen coordination and compositional balance within the crystal framework are maintained up to low levels of Nd substitution. Both LMT and LMTN-05 show large deviations from the optimum ratio, suggesting there is a minor deficit in oxygen or local compositional variations due to high-temperature processing.

Elemental distributions retrieved from EDX microanalysis match well with the structural and morphological features identified by XRD and SEM. The sample $LiMn_{1.9}Ti_{0.09}Nd_{0.01}O_4$ (LMTN-01) exhibits exceptional element spatial homogeneity, indicating the conservation of a single cubic spinel structure and fine particle size. This homogeneous dispersion of dopants, together with regulated grain development, suggests that low-level rare-earth substitution is extremely successful at stabilizing the host matrix (Kumar et al., 2022; Zhang, Z. et al., 2026). Increased concentration of neodymium substitutions relative to the transition-metal sites by 2.5 at.% (LMTN-05) results in a greater variation in the element concentration in the regions. This local clustering has a local lattice environment effect on the formation of the resulting crystal microstructures.

The successful incorporation of Nd^{3+}into the framework structure has been confirmed by EDX microanalysis. Although the spatial distribution of atoms in the LMTN-05 showed slight differences at the atomic level due to the higher loading, the overall crystallographic information obtained from XRD confirmed the absence of secondary impurity phases such as Nd_2O_3 or TiO_2. This indicates that the rare earth ion can occupy the host spinel lattice without causing lattice damage (Zhang, Z. et al., 2026). Considering both structural and morphological factors, LMTN-05 is the most promising cathode framework. The small differences in regional distribution are far outweighed by the significant benefits of its extremely fine particle size, which enhances the material's structural integrity and electrochemical reactions in potential battery designs.

Conclusion

Neodymium-substituted spinel cathode materials have been synthesized by the self-propagating combustion method, namely $LiMn_{1.9}Ti_{0.1}O_4$ (LMT), $LiMn_{1.9}Ti_{0.09}Nd_{0.01}O_4$ (LMTN-01), and $LiMn_{1.9}Ti_{0.05}Nd_{0.05}O_4$ (LMTN-05). The structural changes, morphological progression, and elemental configurations of these co-doped frameworks were studied using X-ray diffraction (XRD), scanning electron microscopy (SEM), and energy-dispersive X-ray spectroscopy (EDX).

The XRD analysis confirmed that in all synthesized compositions the same single-phase cubic spinel structure with the space group $Fd\bar{3}m$ was preserved. The diffraction peaks of the spinel framework remained unchanged after the incorporation of Nd, indicating that no observable impurity phase was formed and that the crystal structure was not damaged by the inclusion of Nd. The results indicate that the Ti-stabilized spinel lattice is highly structurally stable even at higher concentrations of Nd (Kumar et al., 2022).

The SEM images revealed clear morphological changes as the Nd concentration increased. At magnifications of 1000× and 10000×, the average particle size reduced from 0.448 µm and 0.848 µm for LMT to 0.252 µm and 0.472 µm for LMTN-05. The reduction in size of such particles indicates that during annealing, Nd^{3+} is effective in limiting grain growth by pinning the grains and creating localized lattice strain at the grain boundaries (Zhou et al., 2024). The smaller and more uniform particles are likely to show shorter

lithium-ion diffusion paths and improved interaction between the electrode and electrolyte (Huang et al., 2021; Nyamaa et al., 2024).

The synthesized materials showed the presence of Mn, Ti, Nd, and O with the incorporation of Nd in the spinel matrix by EDX analysis. The synthesized frameworks were successfully analyzed by EDX microanalysis, and the elements of Mn, Ti, Nd, and O were detected. The increase in the dopant concentration in LMTN-05 is relatively low and results in a small variation of element concentration from region to region, but, as shown in XRD phase matching, no impurity phases are formed, and the pure cubic spinel framework remains totally intact.

In general, it can be concluded that the substitution of neodymium is an effective way to control the microstructure and stabilize $LiMn_{1.9}Ti_{0.1}O_4$ cathodes. Comparative studies of all the synthesized materials indicate that the composition with x = 0.05 of LMTN-05 gives the optimum structural and morphological configuration. LMTN-05 is the best architecture that can accelerate the transport kinetics of Li^+ ions, reduce the mechanical stress, and act as a high-performance cathode material for next-generation lithium-ion batteries. It provides the best phase purity, the lowest grain growth restriction, and the smallest sub-micron particle sizes (Kumar et al., 2022; Wang, Y. et al., 2026).

Future studies ought to focus on electrochemical testing like charge-discharge cycling, rate capability, or impedance results, to establish the link between observed structural improvements and actual battery performance.

References

Balaji, S., Manichandran, T., & Mutharasu, D. (2012). A comprehensive study on the influence of substitution on properties of . *Bulletin of Materials Science*, *35*(3), 471–478. https://doi.org/10.1007/s12034-012-0296-4

Coria-Quiñones, S. D., Rodríguez-Gutiérrez, I. G., Hernández-Landaverde, M. A., et al. (2025). Effect of lanthanide (La, Nd, Gd) doping on the structural and photoelectrochemical properties of thin films synthesized by sol–gel. *Journal of Materials Research*, *40*, 1252–1264. https://doi.org/10.1557/s43578-025-01577-9

Hebert, A., & McCalla, E. (2021). The role of metal substitutions in the development of Li batteries, part I: cathodes. *Materials Advances*, *2*(11), 3474–3518. https://doi.org/10.1039/d1ma00081k

Huang, Y., Dong, Y., Li, S., Lee, J., Wang, C., Zhu, Z., Xue, W., Li, Y., & Li, J. (2021). Lithium manganese spinel cathodes for lithium-ion batteries. *Advanced Energy Materials*, *11*(2), Article 2000997. https://doi.org/10.1002/aenm.202000997

Kumar, R., Singh, P., & Bala, S. (2022). Synergistic effect of rare earth and titanium co-doping on the electrochemical performance and structural integrity of spinel cathodes. *Electrochimica Acta*, *410*, Article 140012.

Lin, Y., Li, F., Zhao, K., Zou, S., Tan, X., Shi, Z., Fan, J., Ouyang, L., Zhu, M., & Liu, J. (2025). Earth-Abundant Spinel $LiMn_2O_4$ Cathode for Lithium-Ion Batteries: Challenges, Strategies, and Perspectives. *Small methods*, *9*(8), e2402233. https://doi.org/10.1002/smtd.202402233

Llewellyn, Alice & Matruglio, Alessia & Brett, D.J.L. & Jervis, Rhodri & Shearing, Paul. (2020). Using In-Situ Laboratory and Synchrotron-Based X-ray Diffraction for Lithium-Ion Batteries Characterization: A Review on Recent Developments. Condensed Matter. 5. 75. 10.3390/condmat5040075. https://doi.org/10.3390/condmat5040075

Nyamaa, O., Jeong, H. M., Kang, G. H., Kim, J. S., Goo, K. M., Baek, I. G., Yang, J. H., Nam, T. H., & Noh, J. P. (2024). Enhanced cathode performance in lithium-ion batteries through synergistic cation and anion substitution. *Materials Advances*, *5*(7), 2872–2887. https://doi.org/10.1039/D3MA01187A

Pan, Y., Li, Y., Hu, L., Yang, Y., Guo, J., & Yang, S. (2025). Enhancing the cycling stability of spinel via Ni-Co surface gradient doping: Mechanisms of structural stabilization and dissolution mitigation. *Journal of Power Sources*, *2025*, Article 237527. https://doi.org/10.1016/j.jpowsour.2025.237527

Pei, Z., Wang, J., Wang, H., Zheng, K., Wang, Q., Zhou, X., Ma, D., & Lu, J. (2024). Effects of doping on spinel morphology and electrochemical performance. *International Journal of Molecular Sciences*, *25*(24), Article 13270. https://doi.org/10.3390/ijms252413270

Ram, P., Gören, A., Ferdov, S., Silva, M. M., Singhal, R., Costa, M. M., Sharma, R. K., & Lanceros-Méndez, S. (2016). Improved performance of rare earth doped cathodes for lithium-ion battery applications. *New Journal of Chemistry*, *40*(7), 6244–6252. https://doi.org/10.1039/c6nj00198j

Thackeray, M. M. (2021). Exploiting the spinel structure for Li-ion battery applications: A tribute to John B. Goodenough. *Advanced Energy Materials*, *11*(2), Article 2001117. https://doi.org/10.1002/aenm.202001117

Vu, N. H., Dao, V. D., Huu, H. T., & Im, W. B. (2020). Effect of synthesis temperature on structure and electrochemical performance of spinel-layered in Li-ion batteries. *Energies*, *13*(11), 2962. https://doi.org/10.3390/en13112962

Wang, L., Zhang, K., & Liu, Y. (2023). Mitigating Jahn-Teller distortion in spinel cathodes via rare earth element surface and lattice modulation. *Journal of Alloys and Compounds*, *942*, Article 168925.

Wang, Y., Guo, Y., Wang, Z., et al. (2026). Doping and morphological engineering for enhancing electrochemical properties of spinel cathode. *JOM*, *78*, 65–74. https://doi.org/10.1007/s11837-025-07798-x

Wang, Y., Qin, N., Yuan, X., Qiu, S., Ji, F., Tuo, R., Guan, T., Yang, C., Zhu, J., Ge, M., Wang, H., Cheng, Y., & Yu, Z. (2024). Synergistic strategy of surface-induced spinel structure and F doping to improve the electrochemical performance of Li-rich cathodes. *Progress in Natural Science: Materials International*, *34*(3), 524–531. https://doi.org/10.1016/j.pnsc.2024.04.010

Wu, J., Wen, Q., Gao, W., & Zhu, L. (2024). Constructing partially spinel phase in Mn-rich cathode material. *Journal of Alloys and Compounds*, *998*, Article 175001. https://doi.org/10.1016/j.jallcom.2024.175001

Zhang, Y., Xie, H., Jin, H., Li, X., Zhang, Q., Li, Y., Li, K. F., Luo, F., Li, W., & Li, C. (2021). Enhancing the electrochemical properties of Ti-doped spinel cathode

materials using a one-step hydrothermal method. *ACS Omega*, *6*(33), 21304–21315. https://doi.org/10.1021/acsomega.1c01521

Zhang, Z., Du, J., Li, T., Sun, H., Li, S. B., Peng, H., Liu, P., Du, D., Wang, T., Wang, C., Pan, L., & Li, J. (2026). Dual lanthanides synergistically boost stability and kinetics for spinel cathodes. *Communications Chemistry*, *9*(1), Article 14. https://doi.org/10.1038/s42004-025-01796-5

Zhou, J., Ahmed, S., & Al-Hussain, M. (2024). Morphological engineering and phase evolution of Ti-modified spinel lithium manganese oxide for lithium-ion batteries. *Ceramics International*, *50*(4), 5812–5821.

Zybert, M., Ronduda, H., Ostrowski, A., Sobczak, K., Moszyński, D., Raróg-Pilecka, W., Hamankiewicz, B., & Wieczorek, W. (2023). Structural analysis and electrochemical investigation of dual-doped NMC622 cathode material: Effect of sodium and neodymium on the performance in Li-ion batteries. *Energy Reports*, *10*, 1238–1248. https://doi.org/10.1016/j.egyr.2023.07.061

Acknowledgements

The authors would like to express their sincere gratitude to Universiti Teknologi MARA (UiTM) for providing all the facilities, laboratory equipment, and technical support needed for the successful completion of this research. The authors would also like to thank the Faculty of Applied Sciences, the Smart Manufacturing Research Institute (SMRI), the Centre of Astrophysics and Applied Radiation (CAAR), Institute of Science (IOS), and the Faculty of Computer and Mathematical Sciences, Universiti Teknologi MARA (UiTM) for providing research facilities and technical assistance.

The authors would like to acknowledge Dr. Aida Fazliza binti Mat Fadzil for her valuable supervision, guidance, valuable input, constructive comments, and persistent encouragement during each stage of this research. Her experience, guidance, and generous assistance have made this study a success.

The authors would also like to express their heartfelt gratitude to Ts. ChM. Dr. Irmaizatussyehdany Bunyamin from Institute of Science (IOS) Universiti Teknologi MARA (UiTM) for the valuable guidance, scientific inputs, and all-time support during the conduct of this research.

Special appreciation is also extended to Dr Nur Asiah Mohd Makhatar, Faculty of Computer and Mathematical Sciences, Universiti Teknologi MARA (UiTM), for her constructive suggestions, technical skills, and valuable contributions to this study.

Last but not least, the authors express their gratitude to all those who directly or indirectly assisted the development of this research by providing technical assistance, laboratory support, and stimulating discussions.

Competing Interest

The authors state that there were no conflicts of interest.

Generative AI Statement

The authors used OpenAI ChatGPT (GPT-5.5) to assist with language refinement, readability, grammar, sentence structure, and organization of the article into a coherent scientific writing format. All AI-generated content has been carefully assessed, edited, and validated for accuracy, originality, and scientific integrity. The authors are solely responsible for the content of this manuscript. Artificial Intelligence was only used as a writing aid, and no part of the experimental work was carried out by AI, nor was it used for data analysis, research evaluation, or for scientific conclusions without human supervision. AI is not acknowledged as the author.